Proceedings of BALTTRIB'2024 edited by prof. J. Padgurskas
eISSN 2424-5089 (Online)
DOI: 10.15544/balttrib.2024.8.

CAVITATION EROSION OF 3D PRINTED MARAGING STEEL

T. Lazović*[1], P. Ljubojević*, M. Dojčinović**
*Faculty of Mechanical Engineering, University of Belgrade, Serbia
**Faculty of Technology and Metallurgy, University of Belgrade, Serbia

Abstract: We are witnessing the expansion of the application of metal machine parts and elements obtained using some of the additive manufacturing technologies. However, there are still not many publications on the surface load-carrying capacity of 3D-printed parts, especially worn by cavitation erosion. If cavitation occurs in the fluid that is in contact with the surfaces of machine parts, erosive wear may occur due to high-cycle fatigue of local micro volumes. The result is a loss of material mass and a change in the geometry of the surfaces. In this way, the functionality of the parts, operational ability, load-carrying capacity, service life, and reliability were reduced. The degree of surface damage of machine parts exposed to cavitation depends on the chemical composition, microstructure, and mechanical and anti-corrosion properties of the material. This paper presents the results of testing the resistance to cavitation of metal samples produced on a 3D printer by laser sintering of high-quality steel powder of maraging steel MS1.

Keywords: cavitation erosion, 3D printed metal, maraging steel, MS1

1. INTRODUCTION

Cavitation erosion is a significant issue, particularly in hydraulic machines and systems exposed to variable pressure fluid flow, including components such as valves [1-3], gears [4-6], and sliding and rolling bearings [7-12]. Under certain fluid flow conditions, numerous cavitation bubbles form and implode, creating shock waves that cause fatigue in localized microvolumes on the surfaces of machine parts. This leads to the separation of material, ie. erosional wear resulting in mass loss. Cavitation compromises the integrity of working surfaces and alters the geometry of worn machine parts. The extent of damage and surface degradation caused by cavitation depends on the chemical composition, microstructure, mechanical properties, and anti-corrosion characteristics of the materials from which these components are made. Investigating the nature of the cavitation phenomenon is a major challenge for conventionally manufactured materials and parts made using traditional technologies. However, this issue becomes entirely new when dealing with machine parts produced through additive manufacturing, such as 3D printing. The development and application of these new production technologies have created the need for research into the behavior of machine materials and parts, particularly due to their novel microstructures. There are relatively few publications on the surface load capacity of 3D-printed parts, especially concerning cavitation erosion wear in 3D-printed metals. This paper presents the results of cavitation erosion tests on metal samples produced by laser sintering high-quality steel powder (MS1) on a 3D printer.

Keywords: cavitation erosion, 3D printed metal, maraging steel, MS1.

2. EXPERIMENTAL

The cavitation resistance test was performed in accordance with the ASTM G32-16 standard [13]. This standard test method involves inducing cavitation damage on sample surfaces due to the high-frequency impact of the fluid (water) in which the samples are immersed. During experiment, cavities are formed by the vibration of the exciter, which is also immersed in the fluid. The collapse of these

[1] Author for contacts: Prof. dr. Tatjana Lazović
E–mail: tlazovic@mas.bg.ac.rs

cavities generates periodic microshocks on the surface layer of the sample. As a result, microfatigue occurs in the surface layers, leading to material loss and erosive wear. The laboratory equipment used for cavitation damage testing, along with its main specifications, is listed in Table 1. The model of the testing device (referred to as the "apparatus" in the standard) is shown in Fig. 1.

Table 1. Used laboratory equipment

Device		Note
Cavitation apparatus	Branson Ultrasonics JP40022	Vibration frequency 20 ± 0.5 kHz, horn displacement amplitude 50 µm.
Hardness tester	Microdur MIC 10 (ZwickRoell)	Vickers indenter (136º pyramid diamond
Surface roughness tester	Surtronic Duo II (Taylor Hobson)	Gauge resolution 0.01 µm
Analytic balance	Mettler Toledo	Accuracy of ±0.01 mg

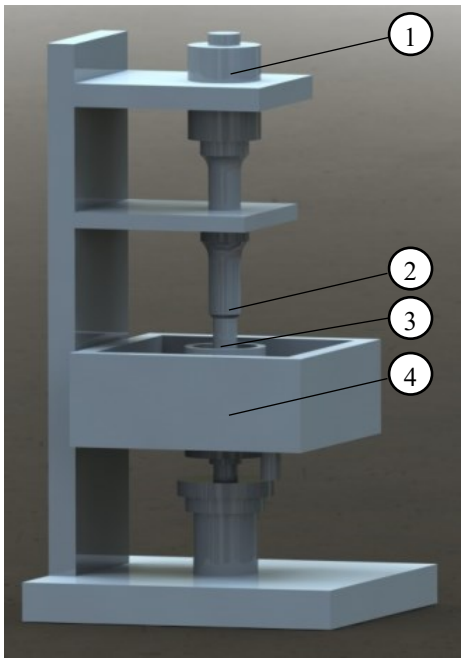

Figure 1. Testing device (1 – transducer, 2 – horn, 3 – test sample, 4 – cooling water bath)

The test samples have a button shape (Figure 2) and were produced using a 3D printer, the M280 DMLS (EOS). The material used for the samples is maraging steel MS1 powder (1.2709 steel; 18% Ni Maraging 300; AISI 18Ni300). The size of the powder particles ranges from 40 to 60 µm. This steel has excellent mechanical properties and is easily heat-treatable using a simple thermal age-hardening process to achieve exceptional hardness and strength. It is ideal for various tooling applications, such as tools for injection molding, die casting of light metal alloys, punching, and extrusion. Additionally, it is well-suited for high-performance industrial and engineering parts, including those used in aerospace and motor racing applications.

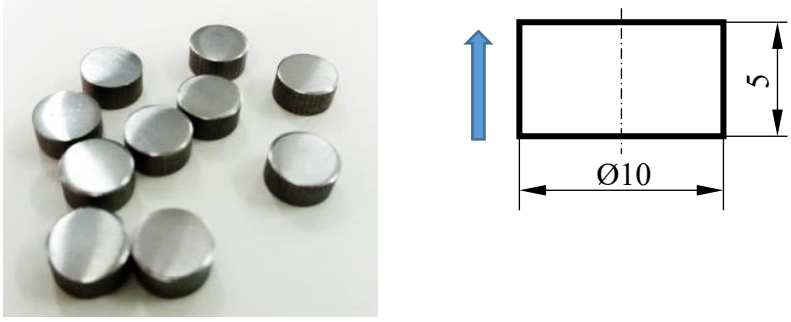

Figure 2. Test samples (arrow shows building direction)

Figure 3 shows the appearance of the sample before the cavitation test, as observed under an optical microscope at various magnifications. Worm-like grain structures are visible across multiple layers at specific angles, which are determined by the manufacturing process. These structures are distinctly separated by layer, and it is clear which structure corresponds to which layer. In the image taken with the highest magnification (500x), both cellular and columnar structures can be identified within different segments, with segment boundaries clearly defining them. The difference between these two structures lies in the grain growth direction, which is influenced by local temperatures at various locations.

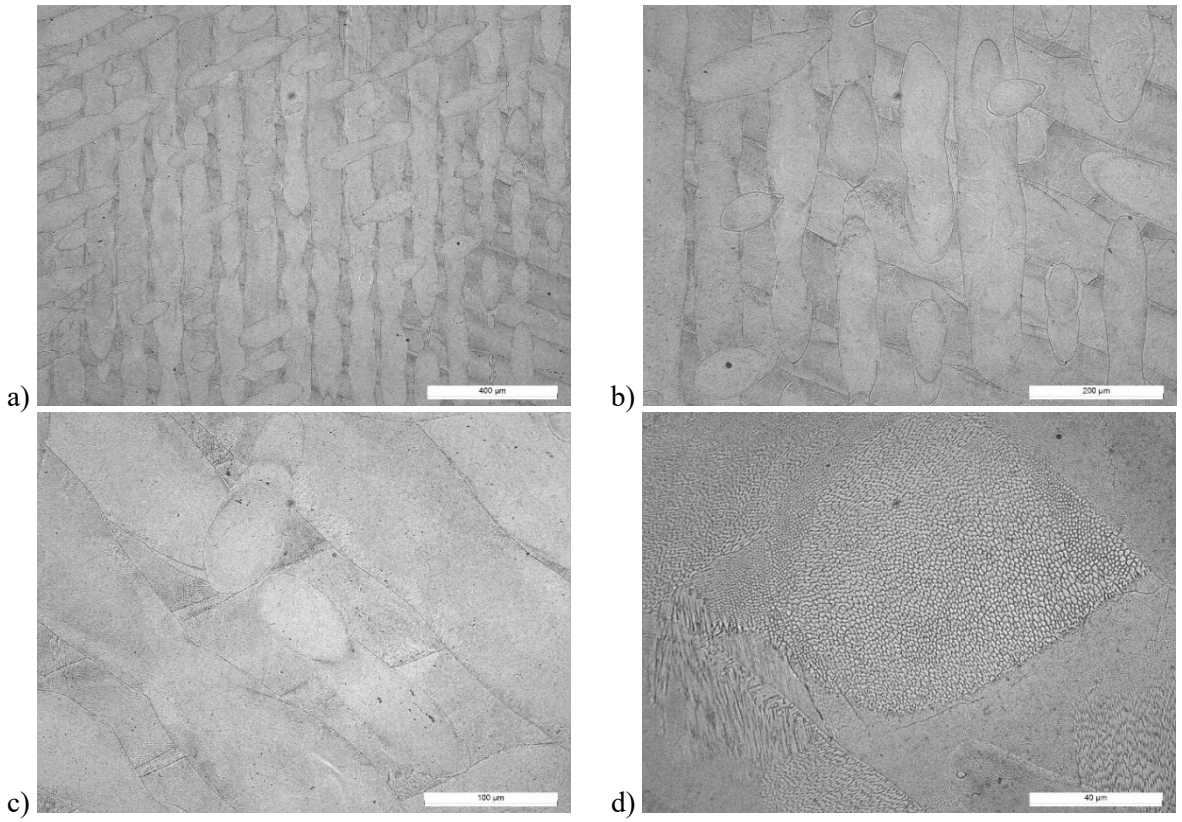

Figure 3. Microscopic images before cavitation erosion (perpendicular to the printing direction) obtained by optical microscopy at the following magnifications: a) 50x; b) 100x; c) 200x; d) 500x.

Figure 4 presents a cross-sectional view of the worm-like structures from the previous image, now viewed in the plane of the construction direction. The segments appear curtain-shaped, and both the cellular and columnar structures are visible in the image at the highest magnification (500x).

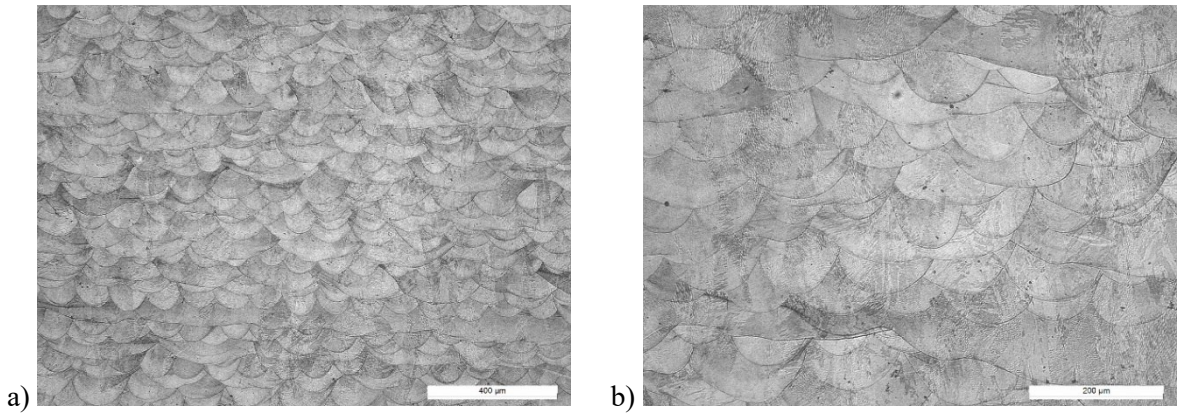

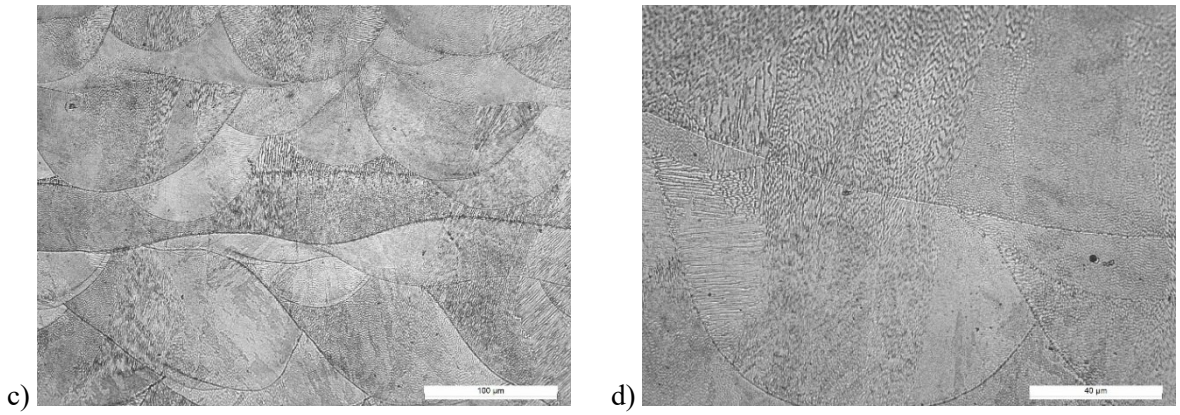

Figure 4. Microscopic images before cavitation erosion (along the printing direction, perpendicular to the layers) obtained by optical microscopy at the following magnifications: a) 50x; b) 100x; c) 200x; d) 500x.

In Figure 5, captured using an SEM microscope, the segment boundaries and the distinction between the cellular and columnar structures are much clearer.

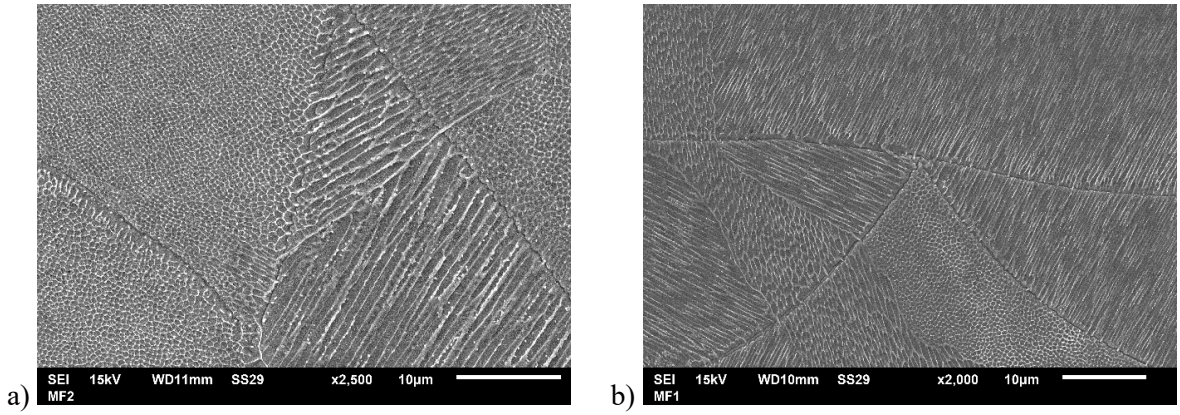

Figure 5. Microscopic images before cavitation erosion obtained by scanning electron microscopy:
a) perpendicular to the printing direction (magnification 2500x); b) along the printing direction, perpendicular to the layers (magnification 2000x).

3. RESULTS AND DISCUSSION

The prepared samples were exposed to cavitation for one, two, and four hours. The mass of the worn samples was measured every half hour, and the mass loss was determined. For each test condition, three measurements were taken to allow for further statistical processing of the results. The study [14] presents a diagram of mass loss over time, from which the rate of change and a cavitation rate of 0.00617 mg/min were determined. Here, we focus on the visual representation of material changes due to cavitation damage, based on the aforementioned test conditions.

The surface of the sample, after varying intervals of exposure to cavitation, reveals the appearance of damage, the size and grouping of which depend on the duration of exposure. After 1 hour of cavitation (a), small, irregularly shaped damages with uneven distribution are observed on the sample. These damages primarily occur at defect sites in the material, which formed during solidification at segment boundaries or in pores containing trapped gas from the working atmosphere. Damages may also appear along surface lines caused by non-ideal polishing. After 2 hours of exposure to cavitation (b), the damage is more widespread and covers a larger portion of the sample surface. Additionally, small grouped damages resembling cellular and columnar structures are visible. After 4 hours of cavitation erosion, the damages are larger (c), with smaller damaged areas seemingly merging to form zones of more extensive damage.

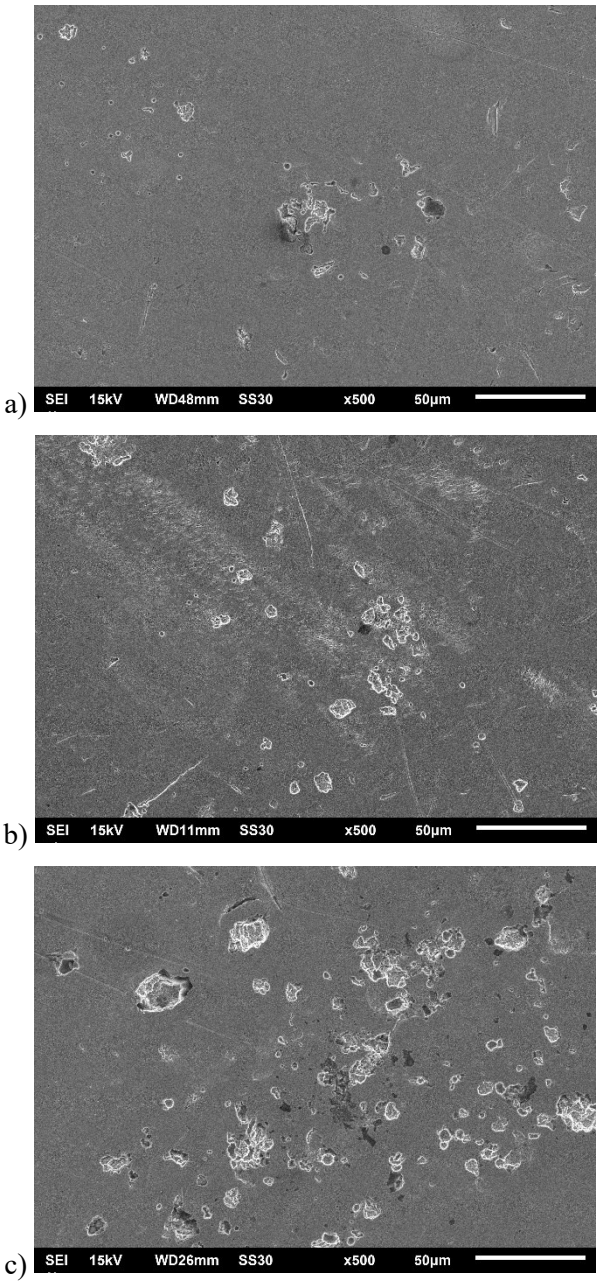

Figure 5. Microscopic images of the worn surface after cavitation erosion obtained by scanning electron microscopy: a) after 1 hour of exposure to cavitation; b) after 2 hours of exposure to cavitation; c) after 4 hours of exposure to cavitation.

4. CONCLUSION

The cavitation rate of maraging MS1 steel (a high-strength steel used in additive manufacturing) can vary depending on factors such as surface finish, heat treatment, and the testing environment. While maraging steels like MS1 are known for their excellent strength and hardness, they can still experience cavitation erosion under certain conditions. That is why our further research is focused on determining the cavitation resistance of MS1 steel samples that are thermally processed by aging and mechanically processed by shot peening. Cavitation resistance is also influenced by the material's structure, which in this case is obtained through laser sintering on a 3D printer. The building layers direction is vertical. Future research should also examine horizontal building and building at an angle (for instance 45°) to allow for more detailed conclusions to be drawn. It would also be interesting to record the topography of the eroded surface (e.g., using atomic force microscopy) and attempt mathematical and geometrical modelling of the surface failure process.

ACKNOWLEDGEMENTS

This work was supported by the Ministry of Science, Technological Development and Innovations of the Republic of Serbia (Contracts: 451-03-137/2025-03/200105 and 451-03-136/2025-03/200135) and also by COST Action CA23155 – A pan-European network of Ocean Tribology (OTC).

REFERENCES

[1] Chinyaev I.R., Fominykh A.V., Pochivalov E.A. Method for determining of the valve cavitation characteristics. Procedia Engineering 150 (2016) 260-265.
[2] Jin Z., Gao Z., Qian J., Wu Z., Sunden B. A parametric study of hydrodynamic cavitation inside globe valves. Journal of Fluids Engineering 140, 3 (2018) 031208.
[3] Qian J., Gao Z., Hou C., Jin Z. A comprehensive review of cavitation in valves: mechanical heart valves and control valves. Bio-design manufacturing 2, 9 (2019) 119-136.
[4] Ouyang T., Mo X., Wang J., Cheng L. Numerical investigation of vibration-induced cavitation for gears considering thermal effect. International Journal of Mechanical Sciences 233 (2022) 107679.
[5] Mo X., Wang J., Cheng L., Ouyang T. Numerical prediction of vibration induced cavitation erosion in high-speed gears using erosion risk indicators. Tribology International 179 (2023) 108122.
[6] Ouyang T., Wang J., Mo X., Li Y.. Vibration and cavitation in high-speed gears caused by faults. International Journal of Mechanical Sciences 250 (2023) 10832.
[7] Daniel G.B., Machado T.H., Cavalca K.L. Investigation on the influence of the cavitation boundaries on the dynamic behaviour of planar mechanical systems with hydrodinamic bearing. Mechanism and Machine Theory, 99 (2016) 19-36.
[8] Sun D., Li S., Fei C., Ai Y., Liem R. Investigation of the effect of cavitation and journal whirl on static and dynamic characteristics of journal bearing. Mechanical Science and Technology 33, 1 (2019) 77-86.
[9] Gamaniel S.S., Dini D., Biancofiore L. The effect of fluid viscoelasticity in lubricated contacts in the presence of cavitation. Tribology International 160 (2021) 107011.
[10] Scott D., McCullagh P.J. The effect of residual gas content on the performance of rolling bearing materials. Wear 34 (1975) 227-237.
[11] Meged Y. Bi-Modal Failure Mechanism of Rolling Contact Bearings, Advances in Materials Physics and Chemistry 10 (2020) 230-238.
[12] Meged Y. Ideal Failure Curve of Rolling Contact Bearings. Advances in Materials Physics and Chemistry 10 (2020) 297-303.
[13] ASTM G32. Standard Test Method for Cavitation Erosion Using Vibratory Apparatus. ASTM International, 2010
[14] Ljubojević P., Dojčinović M., Ćitić A., Ćirić-Kostić S., Bogojević N., Lazović T. Cavitation resistance of laser-sintered MS1 steel. Science of Sintering. OnLine-First Issue 00 (2024) 32
https://doi.org/10.2298/SOS240627032L10.